Mechanism for Acivicin Inactivation of Triad Glutamine Amidotransferases†

Sridar V. Chittur, Thomas J. Klem,¶ Cynthia M. Shafer,‡ and V. Jo Davisson*

Department of Medicinal Chemistry and Molecular Pharmacology, Purdue University, West Lafayette, Indiana 47907-1333

Received June 20, 2000; Revised Manuscript Received November 9, 2000

ABSTRACT: Acivicin [(α*S*,5*S*)-α-amino-3-chloro-4,5-dihydro-5-isoxazoleacetic acid] was investigated as an inhibitor of the triad glutamine amidotransferases, IGP synthase and GMP synthetase. Nucleophilic substitution of the chlorine atom in acivicin results in the formation of an imine−thioether adduct at the active site cysteine. Cys 77 was identified as the site of modification in the heterodimeric IGPS from *Escherichia coli* (HisHF) by tryptic digest and FABMS. Distinctions in the glutaminase domains of IGPS from *E. coli*, the bifunctional protein from *Saccharomyces cerevisiae* (HIS7), and *E. coli* GMPS were revealed by the differential rates of inactivation. While the ammonia-dependent turnover was unaffected by acivicin, the glutamine-dependent reaction was inhibited with unit stoichiometry. In analogy to the conditional glutaminase activity seen in IGPS and GMPS, the rates of inactivation were accelerated ≥25-fold when a nucleotide substrate (or analogue) was present. The specificity (k_{inact}/K_i^{app}) for acivicin is on the same order of magnitude as the natural substrate glutamine in all three enzymes. The (α*S*,5*R*) diastereomer of acivicin was tested under identical conditions as acivicin and showed little inhibitory effect on the enzymes indicating that acivicin binds in the glutamine reactive site in a specific conformation. The data indicate that acivicin undergoes a glutamine amidotransferase mechanism-based covalent bond formation in the presence of nucleotide substrates or products. Acivicin and its (α*S*,5*R*) diastereomer were modeled in the glutaminase active site of GMPS and CPS to confirm that the binding orientation of the dihydroisoxazole ring is identical in all three triad glutamine amidotransferases. Stabilization of the imine−thioether intermediate by the oxyanion hole in triad glutamine amidotransferases appears to confer the high degree of specificity for acivicin inhibition and relates to a common mechanism for inactivation.

Glutamine analogues have been the focus of investigation for many years due to the important role of glutamine metabolism in the biosynthesis of numerous essential metabolites (*1*−*4*). Analogues such as (α*S*,5*S*)-α-amino-3-chloro-4,5-dihydro-5-isoxazoleacetic acid (acivicin), 6-diazo-5-oxo-L-norleucine (DON),[1] and *O*-diazoacetyl-L-serine (azaserine) (Figure 1) have been investigated as potential cancer chemotherapeutic agents following reports of increased glutamine utilization by proliferating cells (*4*−*8*). Acivicin is an α-amino acid produced by *Streptomyces sviceus* that contains the unusual dihydroisoxazole ring as a mimic of the glutamine γ-carboxamide group. The cellular cytotoxicity displayed by acivicin has been attributed to the potent inhibition of glutamine utilization in purine and pyrimidine metabolism (*4*, *7*, *8*). Acivicin has traditionally been classified along with DON and azaserine as simple affinity analogues of glutamine amidotransferases (GATs) (*4*, *5*, *7*). An active site cysteine residue in several GATs displaces the chlorine atom in acivicin resulting in irreversible inactivation of the enzyme (*9*−*12*). While acivicin is considered a potent in vivo inhibitor of GATs in purine and pyrimidine biosynthesis, the molecular basis for this specificity is poorly understood (*13*−*18*). Our studies described here show that acivicin is a highly specific probe for GATs and that its mechanism of inhibition is distinct from the irreversible inhibition demonstrated by other glutamine analogues such as DON and azaserine.

All amidotransferases in the triad subfamily of GATs have a high degree of sequence homology in their glutaminase active sites (*19*). A feature common to many of the GATs is the tightly controlled hydrolytic turnover of glutamine expressed by the glutaminase k_{cat} in the presence or absence of ammonia-acceptor substrates (*12*, *19*, *20*). Structures of

† Taken in part from the Ph.D. dissertation of Thomas J. Klem (1996) Purdue University. This project was supported by NIH Grants GM 45756 and an award from the Purdue Cancer Center to V.J.D. and GM19405 to C.M.S.

* To whom correspondence should be addressed.

¶ Current address: Department of Food Science, Stocking Hall, Cornell University, Ithaca, NY 14853-7201.

‡ Current address: Chiron Corporation, 4560 Horton Street, Emeryville, CA 94608-2916.

[1] Abbreviations: Acivicin, (α*S*,5*S*)-α-amino-3-chloro-4,5-dihydro-5-isoxazoleacetic acid; DON, 6-diazo-5-oxo-L-norleucine; GAT, glutamine amidotransferase; GMPS, guanosine monophosphate synthetase; AS, anthranilate synthase; CPS, carbamoyl phosphate synthetase; IGPS, imidazole glycerol phosphate synthase; FGAMS, formylglycinamide ribonucleotide synthetase; AICAR, 5′-(5-aminoimidazole-4-carboxamide) ribonucleotide; DTT, dithiothreitol; EDTA, ethylenediaminotetraacetic acid; PRFAR, N^1-(5′-phosphoribulosyl)-formimino-5-aminoimidazole-4-carboxamide ribonucleotide; 5′-ProFAR, N^1-(5′-phosphoribosyl)-formimino-5-aminoimidazole-4-carboxamide ribonucleotide; XMP, xanthosine 5′-monophosphate; PIPES, 1,4-piperazinediethanesulfonic acid; EPPS, *N*-[2-hydroxyethyl]piperazine-*N*′-[3-propanesulfonic acid]; MES, 2-[*N*-morpholino]ethanesulfonic acid; HEPES, *N*-[2-hydroxyethyl]piperazine-*N*′-[2-ethanesulfonic acid]; CHES, 2-[*N*-cyclohexylamino]ethanesulfonic acid; HPLC, high performance liquid chromatography; RPHPLC, reverse phase high performance liquid chromatography; DIPEAA, diisopropylethylammonium acetate; NMR, nuclear magnetic resonance; FABMS, fast atom bombardment mass spectrometry; HREIMS, high-resolution electrospray ionization mass spectrometry; HRCIMS, high-resolution chemical ionization mass spectrometry.

10.1021/bi0014047 CCC: $20.00
Published on Web 01/04/2001

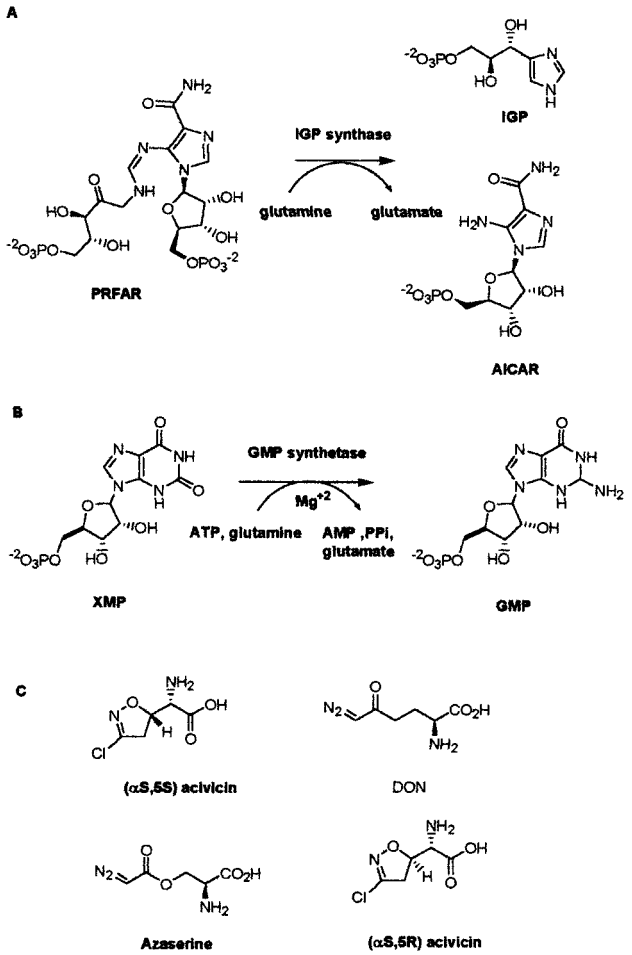

FIGURE 1: (A) Reaction catalyzed by IGPS. (B) Reaction catalyzed by GMPS. (C) Structures of glutamine analogues DON, azaserine, acivicin, and the (α*S*,5*R*) acivicin diastereomer.

three triad GATs, namely, guanosine monophosphate synthetase (GMPS), anthranilate synthase (AS), and carbamoyl phosphate synthetase (CPS), are now available and offer insight into the molecular details of the ammonia transfer step (*21*−*24*). Each of these proteins has unique structural domains for binding of the ammonia-acceptor substrates; however, they share a common fold and conserved active site residues in the glutamine-binding domains. The X-ray crystal structure of substrate bound CPS indicates a solvent-inaccessible tunnel between the glutamine and the ammonia-acceptor substrate binding sites. In GMPS, the amidotransferase domain is separated from the nucleotide-binding domain by 30 Å of solvent-accessible volume in the structure for GMPS. It is assumed that a conformational change occurs upon binding of substrates leading to a transient channel that permits efficient ammonia transfer between the two active sites.

Imidazole glycerol phosphate synthase (IGPS) is also a triad glutamine amidotransferase that catalyzes the formation of IGP and [5′-(5-aminoimidazole-4-carboxamide) ribonucleotide] (AICAR) from [N^1-(5′-phosphoribulosyl)-formimino-5-aminoimidazole-4-carboxamide ribonucleotide] (PRFAR) (Figure 1). This enzyme represents a key juncture between histidine and de novo purine biosynthesis (*25*). IGPS possesses a conserved glutaminase domain like all triad glutamine amidotransferases and a unique synthase domain that binds the acceptor substrate PRFAR. Our investigations of IGPS and GMPS with acivicin and DON were performed as part of the basic characterization of the glutaminase domains of these enzymes. These compounds offer an interesting platform for probing the functional role of the glutaminase and ammonia-acceptor domains. There are several reports that define the inactivation of AS, GMPS, and formylglycinamide ribnucleotide synthetase (FGAMS) by site-specific modification using glutamine affinity analogues (*4*, *7*). However, the type of kinetic information needed to understand the basis for the in vivo specificity of acivicin or the other glutamine analogues are not available. The approach in the present studies focused on the mechanistic distinctions of acivicin and DON in their specificity for the glutaminase binding sites. A comparison of the inactivation profiles in GMPS, the heterodimeric IGPS (HisHF) from *E. coli* and the bifunctional IGPS (HIS7) from *S. cerevisiae* provides a basis for understanding the general aspects of the acivicin specificity in all triad amidotransferases. Kinetic analyses were performed with acivicin and its (α*S*,5*R*) diastereomer to understand the potency and mechanism of acivicin inactivation as it relates to binding orientation. A theoretical model for acivicin inhibition based on the glutaminase domain crystal structure of GMPS is proposed here (*21*). These observations indicate significant roles for the glutaminase oxyanion hole as an electrostatic match for stabilization of the tetrahedral intermediate of acivicin and provide a basis for defining this compound as a highly specific glutamine irreversible inhibitor of triad GATs.

MATERIALS AND METHODS

Materials. Acivicin, DON, and 4-vinylpyridine were obtained from Sigma. L-glutamine was purchased from Aldrich and further recrystallized from 50% ethanol. ATP and organic buffers were purchased from Sigma. Acetonitrile was from Mallinckrodt, triethylamine, diisopropylethylamine, and 1,2-dimethoxyethane (DME) were obtained from Aldrich, and trifluoroacetic acid (TFA) was from Pierce. AG 50W-X8 resin was purchased from Bio-Rad. All solvents were HPLC grade. CH_2Cl_2 was obtained from Mallinckrodt and was distilled from CaH prior to use.

Peptide and protein RPHPLC was performed using Beckman System Gold consisting of an Analog Interface Module 406, Diode Array Detector Module 168, and a Spectra Physics SP8700XR gradient maker. Optical rotations were measured on a Perkin-Elmer 241 polarimeter, and the temperature was controlled by a constant temperature water circulating bath. ^{1}H NMR and ^{13}C NMR spectra were recorded on a Brüker ARX 300 spectrometer. Chemical shifts were referenced to 0.00 ppm (tetramethylsilane in $CDCl_3$) or to 4.80 ppm (the HOD peak in D_2O). ^{13}C NMR spectra were referenced to 77.0 ppm ($CDCl_3$) or externally referenced to dioxane (66.5 ppm) for D_2O samples. ^{13}C multiplicities were deduced from DEPT experiments using the Brüker software.

Chemical Synthesis. (a) (αS,5R)-α-[(Benzyloxycarbonyl)-amino]-3-chloro-4,5-dihydro-5-isoxazoleacetic acid methylidene ester (26). Glyoxylic acid aldoxime (1.55 g, 17.4 mmol) was dissolved in DME (20 mL), and *N*-chlorosuccinimide (4.66 g, 34.9 mmol) was added. The mixture was refluxed until the evolution of CO_2 ceased (∼10 min). After

cooling the sample to room temperature, (2*S*)-*N*-(benzyloxycarbonyl)vinylglycine methylidene ester (1.44 g, 5.81 mmol) in DME (30 mL) was added, followed by $KHCO_3$ (4.10 g, 41.0 mmol) and H_2O (0.5 mL). After stirring the sample at room temperature for 18 h, the reaction mixture was filtered, and the filtrate was concentrated in vacuo. The resulting yellow solid was dissolved in EtOAc, and the organic layer was extracted twice with brine. The brine layers were back-extracted with EtOAc, and the organic layers were combined, dried through $MgSO_4$, and concentrated to a yellow oil (3.65 g). Column chromatography followed by normal phase HPLC (Dynamax Macro Silica Column, 4.9 mL min^{-1}, 15% EtOAc/hexane to 85% EtOAc/hexane over 60 min; λ 254 nm) gave two diastereomers [(α*S*, 5*R*): 47.5 min; (α*S*, 5*S*): 49.6 min] in a combined yield of 53% (0.99 g) and a ratio of 1:1.5. (α*S*, 5*R*): 0.41 g; $[\alpha]_D$ −2.6° (c 1.41, $CHCl_3$); IR (NaCl, neat) 1800, 1715 cm^{-1}; ^1H NMR (300 MHz, $CDCl_3$) δ 3.36 (m, 1 H), 3.60 (m, 1 H), 4.49 (bs, 1 H), 5.23 (m, 4 H), 5.70 (bs, 1 H), 7.37 (m, 5 H); ^{13}C NMR ($CDCl_3$) δ 40.3 (CH_2), 58.5 (CH), 68.6 (CH_2), 79.1 (CH_2), 81.4 (CH), 128.2 (CH), 128.7 (CH), 134.8 (C), 150.0 (C), 154.3 (C), 169.4 (C); HREIMS found *m*/*z* 324.0508 (M^+), $C_{14}H_{13}N_2O_5Cl$ requires 324.0513.

*(b) (α*S*,5*R*)-α-Amino-3-chloro-4,5-dihydro-5-isoxazoleacetic acid (27).* (α*S*,5*R*)-α-[(Benzyloxycarbonyl) amino]-3-chloro-4,5-dihydro-5-isoxazoleacetic acid methylidene ester (0.34 g, 1.04 mmol) was dissolved in CH_2Cl_2 (5 mL) and cooled to 0 °C. A solution of BCl_3 in CH_2Cl_2 (5.2 mL, 5.2 mmol) was added to the solution over 1 min. After 2.25 h, the reaction was quenched with water, and the organic layer was extracted twice with water. The aqueous layer was concentrated in vacuo to give a brown solid. The crude material was dissolved in 2 M HCl and placed on a cation exchange column (AG 50W-X8 resin equilibrated with 2 M HCl) and eluted with H_2O and then NH_4OH (0.5 M). The ninhydrin positive fractions were lyophilized and further purified by RPHPLC (0.1% TFA in H_2O, 7 mL min^{-1}, λ 254 nm; retention time 16.3 min) to give a white solid (40.1 mg, 22%). $[\alpha]_D^{22}$ −83.3° (c 0.4, H_2O); lit. value (*28*) $[\alpha]_D^{22}$ −109° (c 1.12, H_2O); IR (NaCl, neat) 3450 (NH), 3000 (COOH), 1735 (C═O), 1685 (C═N) cm^{-1}; ^1H NMR (300 MHz, D_2O) δ 5.18 (ddd, 1 H, J = 10.5, 7.6, 7.5 Hz), 4.05 (d, 1 H, J = 7.6 Hz), 3.63 (dd, 1 H, J = 18.3, 10.5 Hz), 3.48 (dd, 1 H, J = 18.3, 7.5 Hz); ^{13}C NMR (D_2O) δ 41.9 (CH_2), 56.4 (CH), 80.2 (CH), 152.8 (C), 170.1 (C); HRCIMS found *m*/*z* 179.0227 (M^+), $C_5H_8N_2O_3Cl$ requires 179.0223; Anal. calcd for $C_5H_7N_2O_3Cl$: C, 33.63; H, 3.95; N, 15.69; Cl, 19.85. Found: C, 33.46; H, 3.76; N, 15.30; Cl, 19.82.

Biochemical Analysis. Recombinant overexpression systems and purification protocols for *E. coli* HisH, HisF, IGPS (HisHF), 5′-ProFAR isomerase (HisA), and GMPS were described earlier (*21*, *25*). A source of recombinant *S. cerevisiae* IGPS (HIS7) was developed and purified as described for use in these studies (*20*). A 25 mM acivicin stock solution was prepared in 50 mM Tris-HCl (pH 8.0) and stored at −80 °C. Acivicin concentrations were determined by UV using Σ^{220} 1998 M^{-1} cm^{-1}. FABMS data was obtained on a Kratos MS50 while high-resolution mass spectral data were obtained on a MAT95XL mass spectrometer at the Purdue University Campus-Wide Mass Spectrometry Center. Protein N-terminal sequencing was conducted at the Laboratory for Macromolecular Structure at Purdue University on an Applied Biosystems Procise 491 microsequencer. All UV−Vis spectroscopy was performed on either a Varian Cary 3 or Varian Cary 4 spectrophotometer equipped with a temperature controller running the Varian Windows software version 1.0(8). Data collections were configured to acquire not less than one point every 0.1 s. Data obtained from all these experiments were analyzed using KaleidaGraph for Windows v3.09 (Synergy software) that uses a Levenberg−Marquardt algorithm for general curve fitting (*29*).

Standard IGPS Activity Assays. The IGPS activity of HIS7 was assayed in a volume of 1 mL containing 50 mM PIPES (pH 7.0), 40 mM glutamine, 100 μM PRFAR at 30 °C (*20*). In some cases, the PRFAR was prepared in situ by incubating 100 μM 5′-ProFAR and 5 μg of 5′-ProFAR isomerase at 30 °C for 10 min. In either case, the reactions were initiated by the addition of 1 μg of HIS7 (18 pmol), and the PRFAR consumption was observed by a decrease in absorbance at 300 nm over 1 min. The assays for the *E. coli* IGPS (HisHF) were carried out in a similar fashion in 50 mM Tris-HCl (pH 8.0) using 50 μM PRFAR, 5 mM glutamine with initiation by addition of enzyme (*25*). In the assays for HisH function, the conditions were identical to those for *E. coli* IGPS except that the HisH (0.5 or 0.72 μg) was added before initiating the reactions with 0.6 μg (20 pmol) of HisF. Experiments to determine the effect on the ammonia-dependent reaction were performed under the same conditions as above except 400 mM NH_4Cl was used as the nitrogen source.

Preincubation Experiments. In 200 μL of 50 mM Tris-HCl (pH 8.0), HisHF (20 μg, 2 μM) was treated with 10−50 μM acivicin or 0.2−4 mM DON at 22 °C. Ten microliter aliquots were analyzed over 30 min using the standard activity assay. For glutamine protection experiments, acivicin was held constant at 180 μM, and glutamine was included in the reaction at 1−20 mM. In a similar manner, HIS7 (24.4 μg, 2 μM) was treated with 10−158 μM acivicin in 200 μL of 50 mM PIPES (pH 7.0). The protection experiments with HIS7 contained 158 μM acivicin and 10−40 mM glutamine.

When elevated glutamine concentrations were used in the IGPS assays, the preincubation mixtures contained 4.3 μg of HisHF (0.43 μM) and acivicin concentrations ranging from 18 to 900 μM in 50 mM Tris-HCl (pH 8.0) at 22 °C. Twenty microliter aliquots were added to the standard PRFAR assay mixtures containing 100 mM glutamine for HisHF. The condition for HIS7 assays used 50 mM PIPES (pH 7.0) as a buffer and the enzyme assays included 250 mM glutamine. Experiments with nucleotides or products were conducted with 45 μM acivicin and 5′-ProFAR (10 μM−1 mM) or IGP (50 μM−12.5mM) in 50 mM Tris-HCl (pH 8.0) in a 200 μL volume at 22 °C.

For determination of the stoichiometry of the acivicin−IGPS complex, in a 200 μL mixture HisHF (10 μg, 1 μM) was treated with 100 μM 5′-ProFAR, 10 μg 5′-ProFAR isomerase, and acivicin at 0.05, 0.1, 0.5, 0.75, or 1 μM in 50 mM Tris-HCl (pH 8.0). After 1 h incubation at 30 °C, 10 μL aliquots were analyzed using the standard IGPS initial velocity assay. For HIS7, the reaction was performed in a similar manner using 12 μg (1 μM) of enzyme in 50 mM PIPES (pH 7.0).

When examining the effect of pH, acivicin was held constant at 180 μM and Tris buffer was replaced by the

Scheme 1

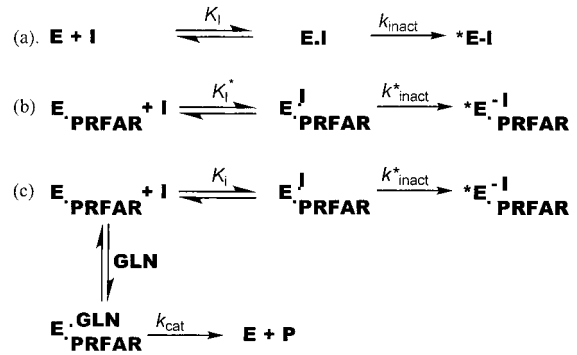

following (at 50 mM): MES (pH 6.0), HEPES (pH 7.0 and 8.0), and CHES (pH 9.0 and 10.0). The effect of temperature on the rate of inactivation was examined by performing the experiments with 180 μM acivicin at temperatures of 4, 15, and 22 °C in a circulating constant temperature water bath.

Kinetic data from these experiments were fit to the simple models in Scheme 1 using nonlinear fits to eq 1 for two-step irreversible inhibition (*30*) where k_{inact} is the maximal rate of inactivation and K_I^{app} is the concentration of inhibitor corresponding to 0.5 k_{inact}.

$$k_{obs} = \frac{k_{inact}[I]}{K_1^{app} + [I]} \quad (1)$$

Acivicin Inactivation of the Glutaminase Subunit (HisH) in E. coli IGPS. In a 200 μL total volume of 50 mM Tris-HCl (pH 8.0), 7.2 μg of HisH was incubated with varied concentrations of acivicin (180−1800 μM) at 22 °C. Twenty microliter aliquots were assayed over 3 h to monitor the rate of subunit inactivation (*25*). The glutamine concentration was increased to 100 mM in the standard PRFAR assay, and the data were analyzed using the methods described above.

Progress Curve Analysis. In a total volume of 1 mL, 50 mM Tris-HCl (pH 8.0), 50 μM 5′-ProFAR, 10 μg of 5′-ProFAR isomerase, 5 mM glutamine, and 1−8.4 μM acivicin or 50−250 μM DON were combined. The cuvette was incubated at 30 °C for 10 min, and the reactions were initiated by the addition of 0.87 μg (17 pmol) of *E. coli* IGPS (HisHF). In the case of HIS7, the reactions were carried out in 50 mM PIPES (pH 7.0) with 40 mM glutamine, and acivicin, DON, and 5′-ProFAR concentrations were increased to 134 μM, 1 mM, and 100 μM, respectively.

Fifty data points were collected over 5 min, during which time the rate was constant as demonstrated by a control reaction lacking acivicin. The data were fit to eqs 2−4 as defined for a competitive irreversible inhibition model (*31*). According to this two-step model (Scheme 1c), the enzyme forms a reversible complex with acivicin followed by irreversible covalent bond formation in the enzyme−acivicin complex. In these equations, v_o represents the initial velocity, V_{max} is the maximum velocity, while K_m is the Michaelis constant for glutamine, S is the substrate concentration, and I is the acivicin concentration. K_i^{app} is the apparent dissociation constant for the inhibitor from the enzyme−nucleotide complex determined at a fixed glutamine concentration.

$$[P] = v_0(1 - e^{-kt})/k \quad (2)$$

$$v_0 = \frac{V_{max}[S]^{Gln}}{K_m^{Gln}\left(1 + \frac{[S]^{Gln}}{K_m^{Gln}} + \frac{[I]}{K_i^{app}}\right)} \quad (3)$$

$$k = \frac{k_{inact}[I]}{K_i^{app}\left(1 + \frac{[S]^{Gln}}{K_m^{Gln}} + \frac{[I]}{K_i^{app}}\right)} \quad (4)$$

Site of Acivicin Modification in the Glutaminase Subunit (HisH) of E. coli IGPS. HisH (23 nmol) was incubated with 100 nmol of acivicin in 50 mM Tris-HCl (pH 8.0) in a total volume of 250 μL at ambient temperature. The reaction was monitored by diluting a 5 μL aliquot 40-fold in the same buffer and analyzing 10 μL of the dilution (containing 0.5 μg of HisH) in the IGPS activity assay. HisH was 90% inactive after 5 h under these conditions. At this point, the mixture was diluted into 1 mL of 8 M urea, 0.1 mM EDTA, 250 mM Tris-HCl (pH 8.5), and 50 μL of β-mercaptoethanol. The mixture was flushed with argon and kept in the dark at ambient temperature for 2.5 h before addition of 4-vinylpyridine (50 μL) and incubation. HisH was separated from lower molecular weight components by gel filtration on a Sephacryl S-100 column (1.5 × 11.5 cm) using 50 mM ammonium bicarbonate (pH 8.0) as the eluent. The recovered protein was dried and dissolved in 100 μL of deionized 8 M urea. To this solution was added 100 μL of water and 200 μL of ammonium bicarbonate (200 mM) before proteolytic digestion with 5 μg of a freshly prepared trypsin solution (in 1 mM HCl). The mixture was maintained under an argon atmosphere for 24 h at 37 °C before RPHPLC analysis.

In a similar manner, 9 nmol of HisHF and 500 nmol of acivicin were incubated in 250 μL of 50 mM Tris-HCl (pH 8.0) at ambient temperature. After 50 min, RPHPLC was performed to isolate the modified HisH subunit and fractions containing the protein were dried in a Speed-Vac concentrator. The recovered protein was dissolved in 80 μL of deionized 8 M urea, 10 μL of 2.5 M Tris-HCl (pH 8.5), 10 μL of 1 mM EDTA, and 5 μL of 5% β-mercaptoethanol before treatment with 4-vinylpyridine and tryptic digestion as described above.

RPHPLC Analysis of Protein Samples. Protein samples were loaded directly onto a Microsorb-MV column (Rainin C4, 300 Å; 0.46 × 5 cm), equilibrated in 20% acetonitrile/0.1% TFA. A gradient to 70% acetonitrile/0.1% TFA at 1 mL min^{-1} was established over 15 min, held for 5 min, and then returned to the starting conditions over 5 min. Acivicin-derivatized HisH eluted at 12.3 min, HisH eluted at 13 min, and HisF eluted at 14.2 min. HisHF diluted into the HPLC eluent dissociated into the two individual subunits as assessed by RPHPLC.

Tryptic Fragment Separation. Tryptic digestions were clarified by microcentrifugation at 14000 rpm for 2 min prior to loading onto an RP-300 Aquapore column (Brownlee C8, 300 Å; 0.46 × 25 cm) in 10% acetonitrile/0.1% TFA. A linear gradient to 60% acetonitrile/0.1% TFA over 90 min at 1 mL min^{-1} was used to elute the peptide fragments. The UV-absorbance of the eluent at both 254 and 280 nm was monitored, and fractions containing the isolated peptides were collected in 1.5 mL eppendorf tubes, dried in a Speed-Vac

concentrator, and stored at 4 °C before amino acid sequence or mass analysis.

GMPS Inactivation Assays. The GMPS activity assay mixtures consisted of 100 mM EPPS buffer (pH 8.5), 20 mM glutamine, 2 mM ATP, 200 μM XMP, 1 mM EDTA, 100 μM DTT, 20 mM $MgCl_2$, and 5−100 μM acivicin (or 50 μM−2 mM DON) in 1 mL total volume. The mixtures were incubated for 4 min at 40 °C in a quartz cuvette before reaction initiation by addition of GMPS (6 nM) in 100 mM EPPS, pH 8.5. The conversion of XMP to GMP was monitored at 290 nm on a Cary 4 spectrophotometer using an extinction coefficient of 1500 M^{-1} cm^{-1}. Progress curves were obtained and analyzed as described above for the IGPS reactions.

Inhibition of IGPS and GMPS by 5R-Acivicin. Steady-state inhibition of HIS7 and GMPS by 5*R*-acivicin was determined using the standard IGPS and GMPS activity assay conditions. The glutamine concentration was varied from 1 to 20 mM, and the initial velocities over the first 1 min were measured with a range of inhibitor concentrations from 50 to 500 μM for HisHF and from 0.1 to 1 mM for GMPS. The data were fitted to steady-state equations for competitive inhibition using a BASIC version of the FORTRAN programs of Cleland (*32*) developed by R. Viola.

Molecular Modeling. All computer simulations were performed on a Silicon Graphics Octane workstation. Models of acivicin and the (αS,5*R*) acivicin were constructed in SYBYL version 6.5 (Tripos Inc, St. Louis, MO) and were energy-minimized with MAXIMIN using the standard settings. The inhibitor model was fit into the glutaminase active site from the crystal structure of GMPS (PDBID 1GPM) (*21*). Acivicin was docked into the active site so that the sulfur nucleophile of Cys 86 was within bonding distance (1.8 Å) to C3 of the dihydroisoxazole ring. The stereochemistry of the cysteine sulfur attack was selected so that the nitrogen of the dihydroisoxazole ring was within hydrogen bonding distance of the backbone nitrogens for Tyr 87 (N−H distance 2.8 Å) and Gly 59 (N−H distance 2.9 Å). The (αS,5*R*) diastereomer was docked in the active site by superimposing the α-amino and carboxyl groups onto the previously docked acivicin. The same procedure was used to dock both compounds in the glutaminase active site of CPS using the published X-ray crystal structure (PDB ID 1A9X) of the active site containing the trapped glutamyl thioester. The atoms of acivicin that were superimposed included C3 of the dihydroisoxazole ring onto the γ-glutamyl carbon as well as the α-amino and carboxyl groups.

RESULTS

IGPS Inactivation by Glutamine Analogues in Preincubation Experiments. Inactivation experiments indicated that both the *E. coli* and the *S. cerevisiae* IGPS were irreversibly inhibited by DON and acivicin, while azaserine (an isosteric analogue of DON) behaved as only a weak reversible inhibitor. DON specifically inhibited the glutamine activity of IGPS with minimal effect on the ammonia-dependent reaction. The DON inactivation process showed pseudo-first-order kinetics over 1 h during which time, the enzyme lost 95% of the glutamine-dependent activity while retaining 85% of the ammonia-dependent activity. Similarly, acivicin did not have any effect on the ammonia-dependent reaction of IGPS. However, in the case of the glutamine-dependent reactions, acivicin inactivation did not exhibit pseudo-first-order kinetics (Figure 2, panel A). Plots of log % activity against time revealed biphasic curves with an initial rapid loss of activity followed by a slower second phase of inactivation. Note that none of the curves intercept the ordinate axis at log 2 (100% activity). Plots of the amplitude of the initial phase (*y*-intercepts) as a function of acivicin concentrations showed a hyperbolic relationship in the case of both the HisHF and the HIS7. In all cases, the enzymes were protected from inactivation by inclusion of glutamine in the preincubation with a rate reduction of ≥50% being achieved at 40 mM glutamine (not shown).

The biphasic character of the inactivation data provoked further experimental variations to probe for a reversal of the initial inactivation phase. The inactivation rates for both phases were maximal in the range of pH 7.0 to pH 8.0 and mirrored the pH dependence of the glutamine-dependent turnover for IGPS activity. Lowering the temperature from 30 to 4 °C slowed the rate of only the second phase, while varying the pH from 6.0 to 10.0 affected the rate of both phases of the inactivation process (not shown) consistent with ionization of a function group in both phases of the inactivation. When 6-fold higher concentrations of glutamine were used in the HIS7 assay, the kinetics of the inactivation approached pseudo-first-order behavior (Figure 2, panel B). Inclusion of 20-fold higher glutamine in the HisHF initial velocity assays showed the same effect on inactivation kinetics. These modified conditions allowed for direct determination of the constants shown assuming the model in Scheme 1a and the data are summarized in Table 1.

Nucleotide Binding and Acivicin Inactivation. A common feature for GATs is the conditional glutaminase activity that can be stimulated by the addition of the second substrate (*19*). In the absence of PRFAR, both DON and acivicin inactivated IGPS at the similar first-order rates especially in the case of HIS7 (Table 1). The kinetic constants determined in the presence of PRFAR assume the simple model in Scheme 1b and show that acivicin inactivation can be stimulated in both HisHF and HIS7. Previous studies had shown that 5′-ProFAR or IGP binding could stimulate the glutaminase activity of IGPS (*20*, *25*). From comparative assays performed under identical conditions, binding of these compounds were found to increase the specificity of DON and acivicin inactivation of *E. coli* HisHF by 4−6-fold and 5−20-fold, respectively (not shown).

The data in Table 1 and the biphasic kinetic behavior observed in the preincubation approach provoked a more complete kinetic model. Upon dilution of the preincubation mixtures into the turnover assay, a parallel branch model is proposed to account for the inactivation data (Scheme 2). The rapid inactivation phase shows a dependence upon glutamine concentration if the pathway(s) to the PRFAR-inactivated complex is faster than dissociation of the inhibitor. Scheme 2 assumes some random sequential binding order of the substrates glutamine and PRFAR but would still be valid if this were a compulsory order binding mechanism. The initial loss of activity would be reversible and increasing glutamine concentrations should trap any free enzyme present. The biphasic aspect of the kinetic behavior reflects the limitations of this approach to analyze acivicin inactivation in this family of enzymes.

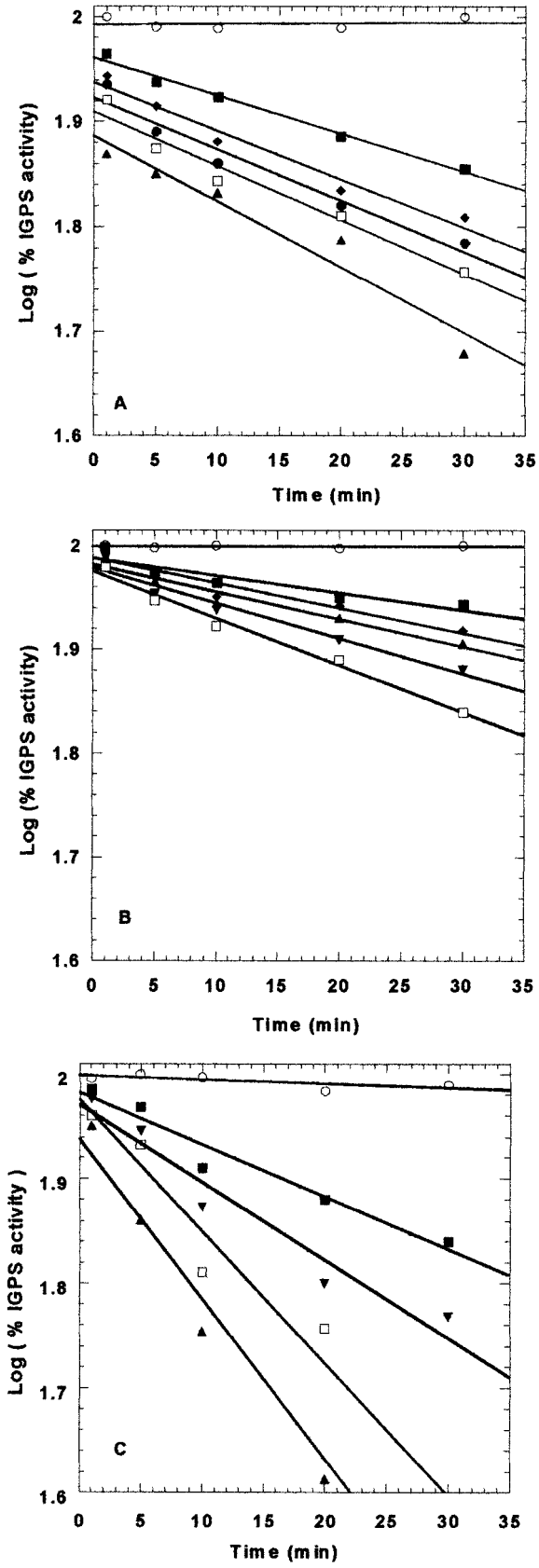

FIGURE 2: (A) Preincubation experiments with HIS7 and acivicin (○) 0 μM, (■) 8.9 μM, (◆) 26.8 μM, (●) 52.5 μM, (□) 105 μM, and (▲) 158 μM with 40 mM glutamine in the initial velocity assays. (B) Preincubation experiments with HIS7 and acivicin (○) 0 μM, (■) 52.5 μM, (◆) 105 μM, (▲) 210 μM, (▼) 420 μM, and (□) 840 μM with 250 mM glutamine in the initial velocity assays. (C) Preincubation experiments with HIS7, 100 μM PRFAR and acivicin (○) 0 μM, (■) 8.9 μM, (▼) 26.8 μM, (□) 52.5 μM and (▲) 105 μM using 250 mM glutamine in the assays.

Table 1: Kinetic Parameters for the Inhibition of IGPS by Acivicin and DON Determined from Preincubation Experiments

enz	inhibitor	effector	K_I^{app} μM	$k_{inact} \times 10^{-2}$ (s^{-1})	k_{inact}/K_I^{app} ($M^{-1}s^{-1}$)
HisHF	acivicin	none	660 ± 50	0.20 ± 0.02	2.7
HisHF	acivicin	50 μM PRFAR	$<9^a$	$\geq 10^a$	$\approx$10000
HisHF	DON	none	3200 ± 300	0.103 ± 0.001	0.32
HisHF	DON	50 μM PRFAR	220 ± 20	3.3 ± 0.3	150
HIS7	acivicin	none	45 ± 6	0.0067 ± 0.0007	1.5
HIS7	acivicin	100 μM PRFAR	5.6 ± 1.1	0.164 ± 0.009	290
HIS7	DON	none	235 ± 31	0.017 ± 0.002	0.81
HIS7	DON	100 μM PRFAR	50.9 ± 6.1	0.023 ± 0.002	4.6

[a] The K_I with PRFAR could not be measured accurately in the bacterial system because the concentrations of acivicin used were similar to the concentration of enzyme and the reaction was no longer pseudo-first-order with respect to IGPS. At 9 μM acivicin (20:1, inactivator/enzyme), the rate of inactivation with PRFAR was too fast to measure with the techniques employed. Assuming 10% of the enzyme was still active at 10 s in the presence of 9 μM acivicin (based on the rate of the reaction at this time point), the k_{inact} can be estimated to be ≥ 0.1 s^{-1}.

Scheme 2

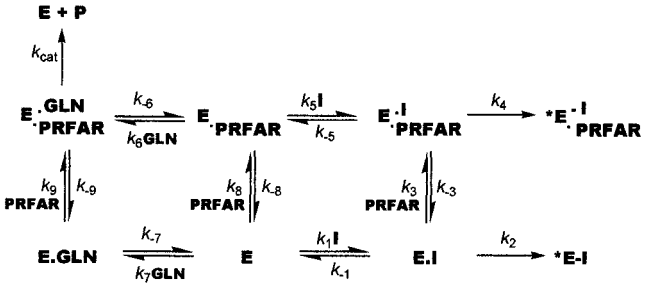

Progress Curve Analysis for DON and Acivicin Inactivation. Analysis of the progress curves for the IGPS reactions offers an approach to assess the kinetic constants for the inhibitors under conditions of competitive turnover that are not possible with conventional initial-rate methods. For HisHF, HIS7, and GMPS, this approach was used to compare the mechanism of inactivation by DON and acivicin. These three enzymes belong to the triad family of GATs and share common structural and catalytic features in the glutamine binding site (*19*, *21*, *22*, *24*). IGPS reaction progress curves were generated in the presence of DON and acivicin and a series are shown in Figure 3. The kinetic constants derived from curve fits of these data are summarized in Table 2 and the steady-state kinetic constants for glutamine turnover by each of these enzymes are provided for comparison in Table 3. Three major points are revealed from the analysis of these data. First, the fact that all three enzymes show a higher specificity for the acivicin when compared to DON is reflected in the relative k_{inact}/K_i^{app} values that are 65−140-fold greater in value. Second, the inactivation process mirrors the catalytic properties of the glutaminase function in each enzyme. In the case of the *E. coli* IGPS activities, the K_i^{app} and k_{inact} values show that the inactivation is 40−80-fold greater in rate than those for the *S. cerevisiae* IGPS, a result that is consistent with the differences in the kinetic specificity for glutamine turnover (Table 3). Finally, the specificity for acivicin is the same as seen for the natural substrate glutamine for each of these enzymes. This factor is one that

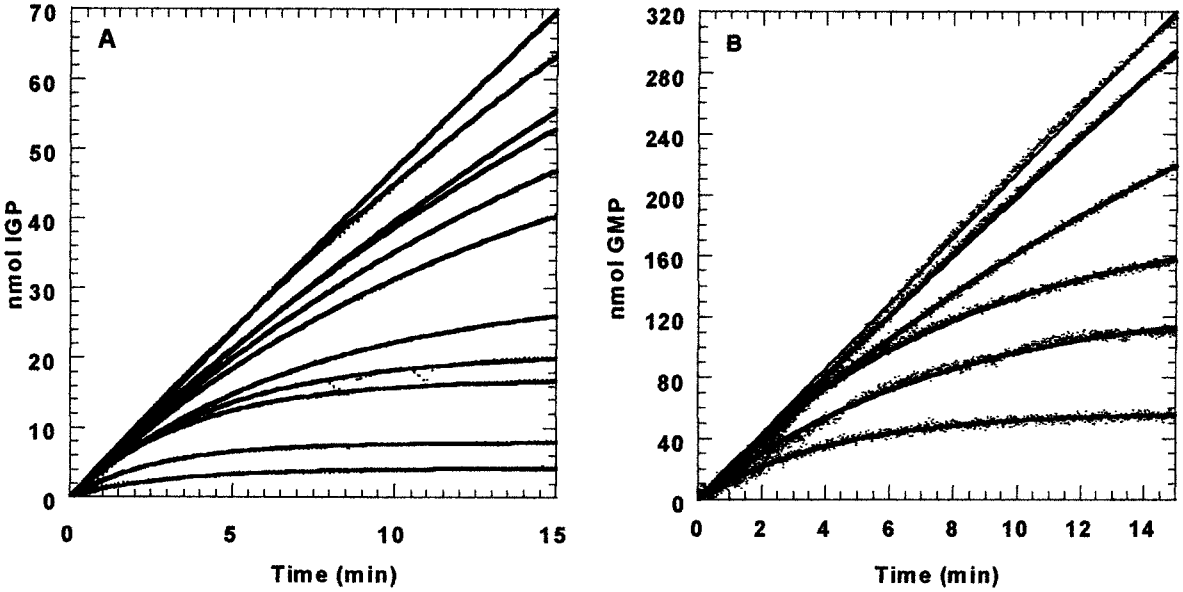

FIGURE 3: Progress curves for IGPS and GMPS reactions. Panel A represents the progress curves for HIS7 at acivicin concentrations of the progress curves for HIS7 at acivicin concentrations of 0, 1.4, 2.8, 4.2, 5.6, 8.4, 17, 25, 34, 67, and 134 μM. Panel B represents the progress curves for GMPS at acivicin concentrations of 0, 5, 10, 40, 50, 100 μM.

Table 2: Kinetic Parameters for the Inhibition of IGPS by Acivicin and DON Determined from Progress Curve Experiments

enzyme	inhibitor	K_i^{app} (μM)	$k_{inact} \times 10^{-2}$ (s^{-1})	k_{inact}/K_i^{app} ($M^{-1}\,s^{-1}$)
HisHF	acivicin	1.5 ± 0.2	6.2 ± 0.70	41000
HisHF	DON	37.6 ± 4.5	2.25 ± 0.17	610
HIS7	acivicin	7.08 ± 0.98	0.75 ± 0.07	1100
HIS7	DON	32.4 ± 3.4	0.025 ± 0.002	7.7
GMPS	acivicin	0.41 ± 0.02	0.72 ± 0.14	18000
GMPS	DON	5.23 ± 0.22	0.14 ± 0.01	270

Table 3: Summary of Steady State Kinetic Constants for the Glutaminase Activity in HisHF, HIS7, and GMPS

enzyme	substrate (or product)	K_m^{Gln} (mM)	k_{cat} (s^{-1})	k_{cat}/K_m^{Gln} ($M^{-1}\,s^{-1}$)
HisHF		4.8	0.07[a]	14.6
HisHF	50 μM PRFAR	0.24	9.1[a]	38000
HIS7		3.5	0.01[b]	1.7
HIS7	100 μM PRFAR	1.7	5.2[b]	3100
GMPS		ND[e]	0.001[c]	
GMPS	AMP, PPi	1.0	22[d]	22000

[a] Klem et al, ref *25*. [b] Chittur et al., ref *20*. [c] Zalkin et al., ref *35*. [d] Deras et al., ref *36*. [e] ND is not determined

clearly differentiates the mechanism of inactivation for this class of GATs by acivicin (see Tables 2 and 3).

The information from the inactivation rates observed in the progress curves are useful in assessing the source of the biphasic kinetics observed in the preincubation experiments and the kinetic model (Scheme 2). The preincubation data show that the initial rapid phase occurs in the initial velocity assay mixtures. Carryover of the free acivicin from the preincubation to the initial velocity assay is a possible contributor to the rapid inactivation phase. Inspection of the progress curve data in Figure 3 for HIS7 at 1.4 μM acivicin reveals that no inhibition occurs over the first 1.5 min. The data in Figure 2, panel A, show that at the highest concentration of acivicin used (corresponding to 1.6 μM when diluted in the enzyme assay) 75% of the enzyme activity remains after a 1-min preincubation. The time it takes to sample and mix the enzyme assay is 15−20 s, and the linear initial velocities were measured over the first 1 min. Under the assay conditions, the rate of inactivation due to the free acivicin would have to be ≥25-fold faster to explain the first 1 min time points observed in Figure 2, panel A. A larger concern for the HisHF enzyme exists since the k_{inact} in the progress curve is 8-fold greater than HIS7. However, the highest concentration of acivicin upon dilution was 0.5 μM and only 60% of the enzyme activity was observed in the preincubation experiments. Using simulated progress curves for HisHF with 0.5 μM (not shown), the amount of inactivation after 1 min is 20%. The rate of inactivation would have to be >3-fold faster to account for the observed data at the highest acivicin concentration and 6-fold greater at the lower acivicin concentrations. Therefore, the rate of inactivation due to the free acivicin carryover from the preincubation experiments to the initial velocity assays could only in part explain the observed initial loss of enzyme activity.

Stoichiometry and Site of Modification in IGPS. The stoichiometry of acivicin inactivation was determined by titration of HisHF and HIS7 activity with limiting amounts of acivicin. Complete inactivation was estimated to be 1.1 mol of acivicin/mol of IGPS in the enzymes from both *E. coli* and *S. cerevisiae*. The HisH subunit of *E. coli* IGPS was also incubated with acivicin and assayed for remaining activity by addition of HisF (K_I^{app} of 4 mM and a k_{inact} of 3.3×10^{-4} s^{-1}). In addition, HPLC analysis of the acivicin treated HisH showed an alteration of the protein retention volume as a function of time. These results were consistent with the acivicin site of modification occurring on HisH at the conserved glutamine-binding site in the triad amidotransferases (*19*).

Tryptic digestion of HisH was predicted to yield 18 peptide fragments with the four cysteines contained in three peptides (Table 4). The conserved cysteine (Cys 77) occurs in fragment 2 that also contains Cys 69. A derivatization protocol was developed to protect cysteine residues against

Table 4: List of Cysteine Containing Peptides after Tryptic Digest of HisH

no.	peptide	residues
1	MNVVILDTGCANLNSVK	1−17
2	ACTQPVLGICLGMQLLGR	68−85
3	LFQGIEDGAYFYFVHSYAMPVNPWTIAQCNYGEPFTAAVQK	129−169

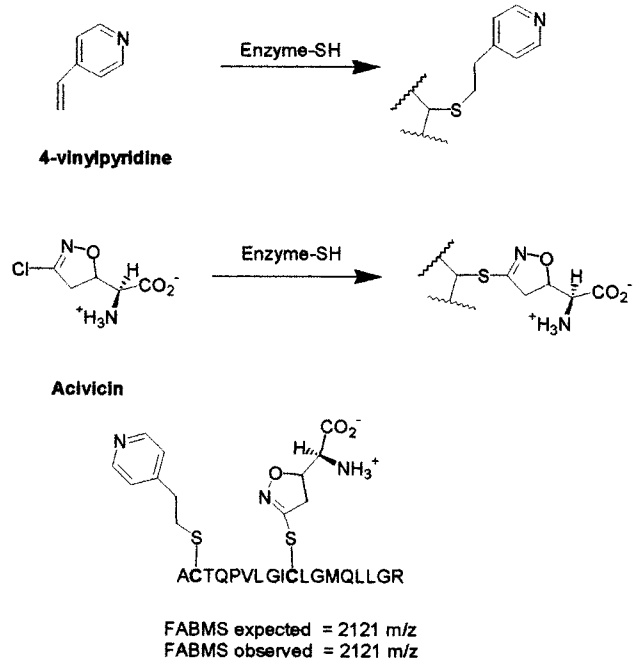

FIGURE 4: Modification of cysteines on HisHF by 4-vinylpyridine and acivicin. Cys 77 is the site of acivicin modification in HisH subunit.

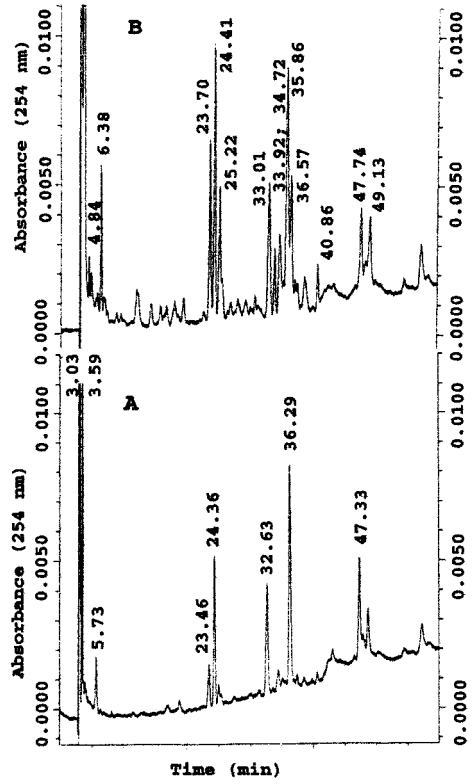

FIGURE 5: RPHPLC chromatograms of tryptic digests of HisH. (A) Without acivicin treatment and (B) with acivicin treatment. Peptide 2, which contains the nucleophilic cysteine 77, eluted at 36.29 min in panel A and at 35.86 min when derivatized (panel B).

decomposition during Edman sequencing (*33*). The modifying group, 4-vinylpyridine, provides an indicative chromophore that enables UV absorbance detection at 254 nm as a means of selecting cysteine-containing peptides by RPHPLC (Figure 4). RPHPLC of HisH using this procedure resulted in the appearance of three unique peaks at 24 min, 32, and 36 min (Figure 5, panel A). Edman sequencing revealed that the peak at 36 min was peptide 2 that contains Cys 77. Modification of the HisH protein by acivicin prior to tryptic digestion resulted in a more hydrophilic peptide 2 that eluted at an earlier retention time (35 min, Figure 5, panel B). Since this peptide contains two cysteine residues, detection of the pyridylethyl derivatized peptide was possible if one residue was masked by acivicin modification. As expected, Edman sequencing showed that the acivicin-modified peptide had a pyridylethyl Cys 69 and an absence of Cys 77. The absence of Cys 77 was attributed to covalent modification by acivicin.

The acivicin-modified peptide 9 was analyzed by positive ion FABMS. The mass of the dipyridylethylated peptide 2 has the expected value of 2084 *m*/*z* and was observed in the control digested HisH. A calculated mass for the peptide containing a pyridylethylated Cys 69 and an acivicin-modified Cys 77 is 2121 *m*/*z*. The parent ion peak obtained from positive ion FABMS had a mass of 2121 *m*/*z*. A second peak at −92 *m*/*z* consistently showed up during analysis and was attributed to the fragmentation of the pyridylethylated cysteine at position 69 to a methionine radical.

Stereochemical Dependence of Acivicin Inactivation. The unusually high degree of acivicin specificity for the triad GATs prompted an analysis of the stereochemistry for acivicin binding at the glutaminase active site. The 5*R*-acivicin diastereomer was synthesized and used as a probe of the inhibitor binding event. Under all conditions, the 5*R*-acivicin behaved like a steady-state inhibitor with respect to glutamine. This compound proved to be a weak reversible competitive inhibitor of HisHF ($K_i = 1.4 \pm 0.02$ mM) and GMPS ($K_i = 0.64 \pm 0.03$ mM).

The inhibitor was docked in the active site of the GMPS glutaminase domain (Figure 7) to create a model for acivicin binding. Superimpositions of the available X-ray crystal structures for GMPS, CPS, and AS indicate that the glutaminase domains of all these enzymes essentially have the same fold with RMS deviations <1.5 Å (*21*−*24*). Therefore, the mechanistic feature of acivicin binding and inactivation in the glutaminase active site is expected to be identical in all the triad GATs. In this model, the oxygen and nitrogen of the dihydroisoxazole ring project into the oxyanion hole defined by the backbone nitrogens of Gly 59 and Tyr 87 in *E. coli* GMPS when the C3 of acivicin is positioned for attack by the nucleophilic Cys 86 (Figure 7). The stabilization of the tetrahedral intermediate formed during acivicin inactivation would be similar to that formed during normal glutaminase action by the enzyme. This unique feature is what contributes to the high specificity of acivicin in all triad

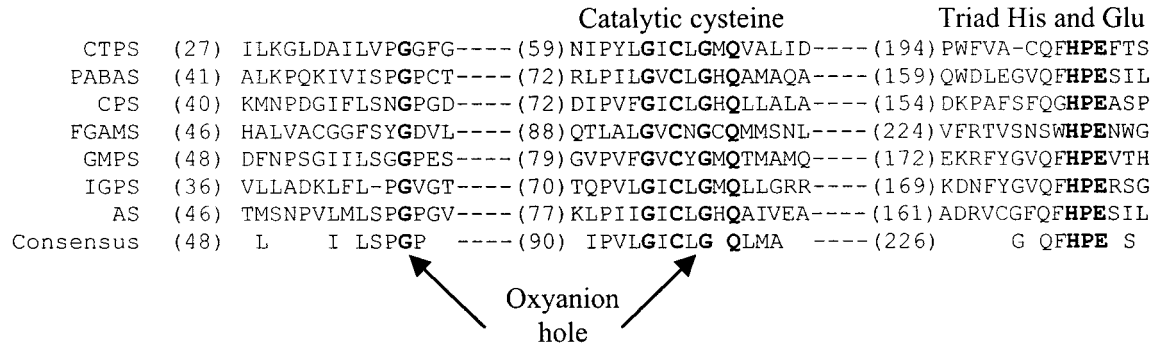

FIGURE 6: Sequence alignments of *E. coli* glutaminase domains from triad GATs using VectorNTI. CTPS = cytidine 5′-triphosphate synthetase, accession #882674; PabAS = *p*-aminobenzoate synthase, accession #129522; AS = anthranilate synthase, accession #2506459; GMPS = guanosine monophosphate synthase, accession #121769; IGPS = imidazole glycerol phosphate synthase, accession #123151; FGAMS = formylglycinamide ribonucleotide synthetase, accession #1788909; CPS = carbamoyl phosphate synthase, accession #115621

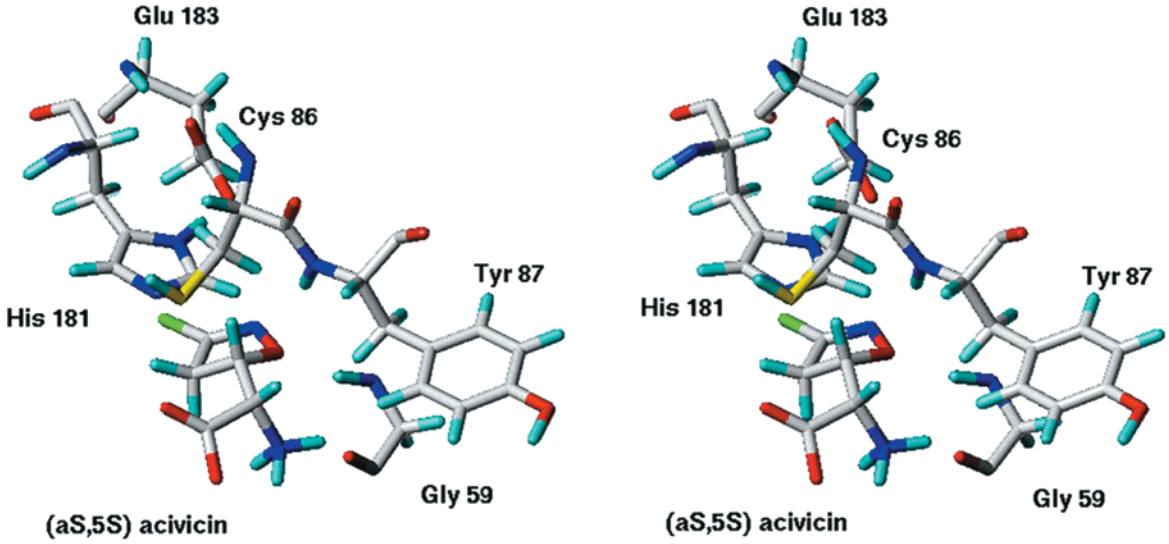

FIGURE 7: (A) Stereoview of the theoretical model for acivicin binding in the glutaminase domain of GMPS with oxygen (red), nitrogen (blue), sulfur (yellow), carbon (gray), hydrogen (cyan), and chlorine (green).

glutamine amidotransferases over simple glutamine affinity analogues such as DON or azaserine. The observation that (α*S*,5*R*) analogue of acivicin was a steady-state inhibitor is consistent with the model (not shown) where the dihydroisoxazole ring is flipped around the axis at C5 and the C3 imine is pointing away from the nucleophilic cysteine in the diastereomer (C3−S bond distance 2.9 Å). As a test of the model, the docking was performed in a distinct data set using coordinates for glutamyl-CPS (*23*). In this case, the constraints on the docking of acivicin were dictated by the positions of the γ-glutamyl carbon in a thioester linkage with the enzyme as well as the critical α-amino and carboxyl groups. What is observed are many functional similarities to the results with the GMPS model. In this case, the residues involved in the oxyanion hole (Leu 270 and Gly 241) are in position to stabilize negative charge on the dihydroisoxazole nitrogen.

DISCUSSION

Acivicin forms an imino-thioether linkage with the conserved active-site Cys 77 of the glutaminase (HisH) domain of IGPS. The site of acivicin modification corresponds to the conserved cysteines of the catalytic triads that define this class of metabolic enzymes (Figure 6). The covalent bonding arrangement has been established by mass analysis in the acivicin modified human GMPS and is assumed for anthranilate synthase (*10*, *12*, *34*). Acivicin inhibition profiles of IGPS and GMPS were fitted to a two-step binding model using progress curve analysis to evaluate the mechanism of action. However, the classical preincubation approach revealed dynamic properties of the enzyme that reflect the highly cooperative functions that occur between the two distinct active sites in these GATs. The biphasic kinetic character of this inactivation process in the preincubation experiments is consistent with the model in Scheme 2 where association of PRFAR with **E·I** and commitment to an inactivated complex is faster than dissociation of acivicin. The binding of acivicin also reflects a strikingly high degree of specificity for the glutaminase active sites of all three enzymes. In fact, the progress curve analyses demonstrate that the specificity of acivicin is equivalent to the substrate glutamine in the presence of nucleotide substrate(s).

The correlations between the glutaminase functions and the mechanism of acivicin inactivation are indicated by these kinetic studies. Stimulation of glutaminase activity in the GATs is a functional property that is especially important in this triad family of enzymes. For instance, the basal glutaminase activity in GMPS is below standard detection limits. Despite the enzyme having active sites that are separated by as much as 30 Å, binding of nucleotide

Scheme 3

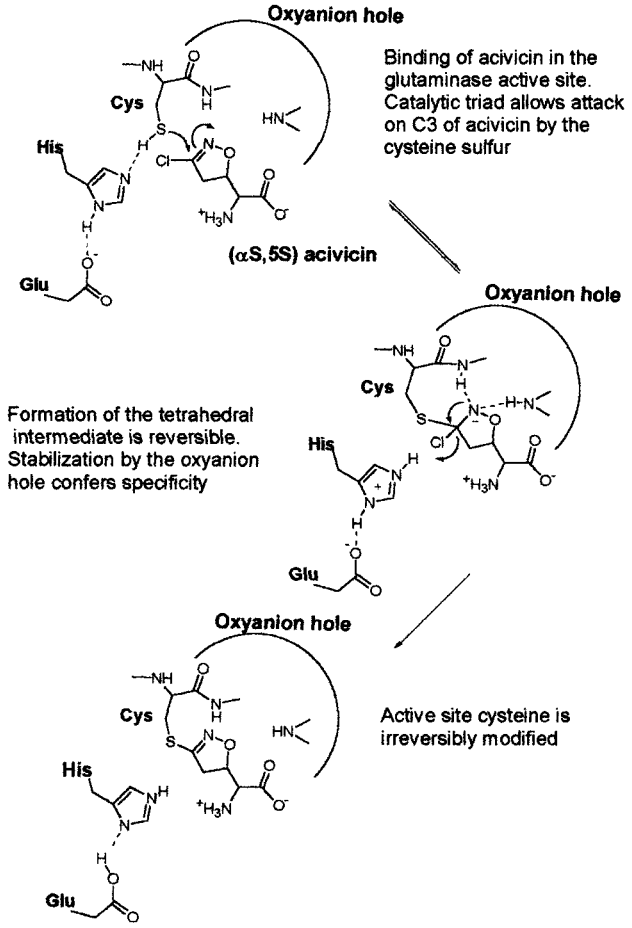

substrates or products in the acceptor domain imparts $\geq 10^4$-fold increase in the glutaminase function (Table 3) (*21*). It is the same factor that is revealed by the kinetics of acivicin inactivation and is attributed to trapping of at least the **E·I** complex by binding of PRFAR. In this context, acivicin is an intriguing mimic whose reactivity is modulated by all the same structural and dynamic features inherent to this family of enzymes.

On a molecular basis (Scheme 3), an explanation for the effect of nucleotide binding would be forward commitment to formation of the covalent product. In the absence of a nucleotide substrate, the bound acivicin partitions slowly to the covalent imino-thioether product. Both steps in Scheme 3 are expected to be sensitive to changes in ionization states of residues in the glutaminase active site consistent with the pH dependence of inactivation rates. At what stage the tetrahedral intermediate is formed on the enzyme is not known, but its stabilization is expected to be the principle factor that enhances the reactivity of this heterocycle through noncovalent interactions. A complimentary electrostatic recognition of the acivicin dihydroisoxazole ring in the glutamine binding site is indicated by a number of observations.

The dihydroisoxazole ring confers to acivicin the specificity for triad GATs. This heterocycle must be uniquely matched to the binding site since other affinity analogues do not bind and react with the same specificity. The importance of this feature is further supported by the acivicin modification of the isolated HisH glutaminase subunit. This is the first case for functional activity in the isolated subunit since glutamine turnover was not observed unless in complex as the HisHF holoenzyme (*25*). In the presence of the nucleotide substrate, the distinctions between DON and acivicin are revealed in the progress curve analysis and the preincubation studies. While both compounds are α-amino acids, the diazoketone group in DON is not a comparable mimic of glutamine showing >100-fold less specificity for GATs. Azaserine, a simple affinity analogue like DON, is a known inhibitor of GATs such as GMPS and FGAMS but does not inhibit IGPS suggesting that the affinity of this compound is dependent upon subtle differences in the glutaminase active sites (*4*, *7*).

The functional and structural similarities of triad glutaminase active sites to those of cysteine proteinases have been previously identified (*19*). A common role for an oxyanion hole in the glutaminase active site would be the stabilization of a reversible tetrahedral intermediate. These features are critical in assessing the structural basis for the specificity of acivicin for the glutaminase active site since the ground state of the chloro-substituted dihydroisozazole ring is resistant to nucleophilic addition under the conditions of the assay. The glutaminase domains of GMPS, CPS, and AS share a common fold (*21*−*23*), and the structural identity of the catalytic triads provides a basis for locating potential residues involved in the oxyanion hole. Amino acid sequence alignments of the glutaminase domains from all the triad amidotransferases (Figure 6) implicate the backbone-NH of two residues playing significant roles in the oxyanion hole. The conserved glycine residue Gly 46 in HisH (Gly 49 in HIS7 and Gly 59 in GMPS) and the NH of the hydrophobic residue following the catalytic cysteine (Leu 78 in HisH, Val 84 in HIS7, and Tyr 87 in GMPS) were found in identical locations when the X-ray crystal structures of the glutaminase domains for the three triad GATs were superimposed. Other residues such as the conserved glycines (Gly 84 and Gly 88 in GMPS) and the hydrophobic residues adjacent to them are expected to contribute to the electropositive features of these oxyanion holes.

The conserved catalytic triad and oxyanion hole structure in the triad amidotransferases define the basis for understanding acivicin recognition. An added experimental basis for assessing the model of acivicin docking in the enzyme active site is provided by the stereospecificity of the inactivation reaction. Only the (α*S*,5*S*) diastereomer of acivicin shows high affinity for both IGPS (HIS7 and HisHF) and GMPS and limits the number of possible binding orientations for any proposed model. Since a crystal structure of IGPS is not yet available, the glutaminase domain of GMPS was used as a starting model for a structural interpretation of acivicin inactivation. The kinetics of acivicin inactivation of the *E. coli* GMPS are similar to IGPS.

Models of the GMPS, CPS, and AS with acivicin docked into the glutaminase active site revealed the role of the key conserved residues in the glutamine binding sites. The oxyanion hole defined by the backbone nitrogens of Gly 59 and Tyr 87 of GMPS stabilize the tetrahedral intermediate formed during inactivation by acivicin through hydrogen bonding in a manner similar to the normal glutaminase mechanism. Both the nitrogen and the oxygen atoms of the dihydroisoxazole ring are within hydrogen bonding distance of these residues. While the location of the α-amino acid

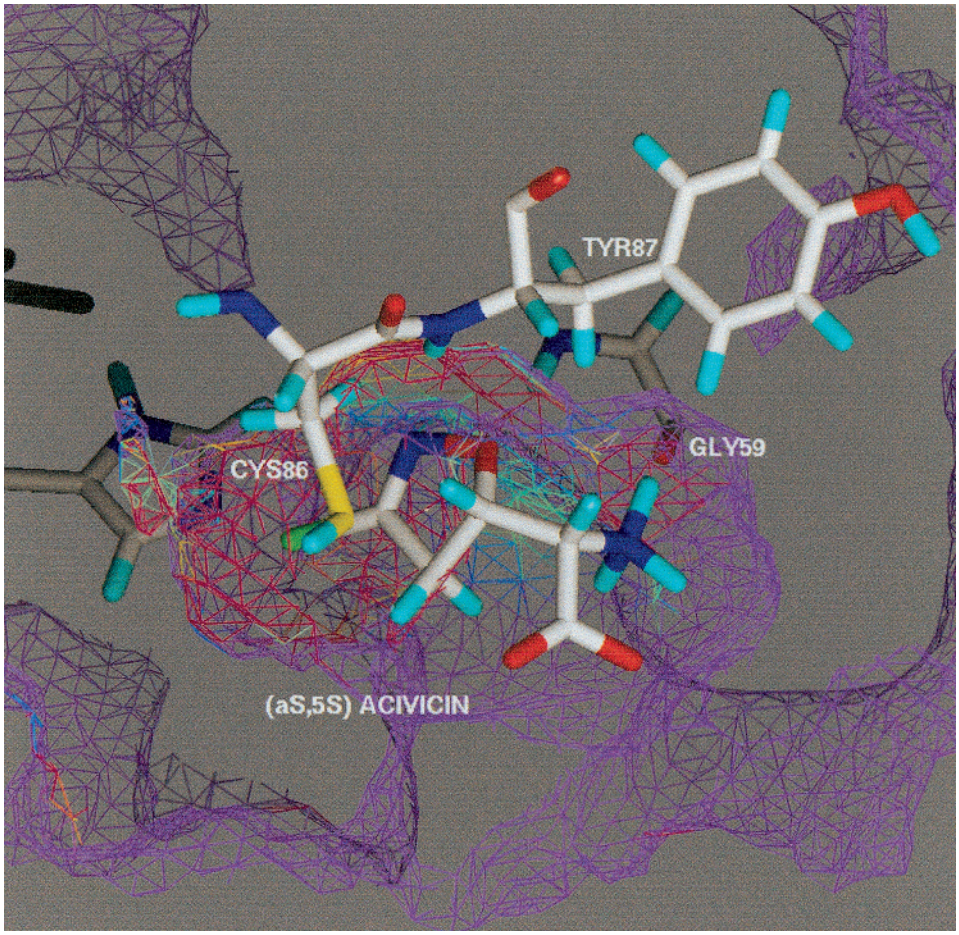

FIGURE 8: Electrostatic potential surfaces for GMPS glutaminase active site and (α*S*,5*S*) acivicin. The negative potential (purple) on the dihyroisoxazole ring is complemented by the electropositive potential (red) surface of the oxyanion hole.

group was not validated in the GMPS structure, the model of the CPS structure used coordinates from crystals with ADP and the trapped γ-glutamyl thioester. The α-amino acid group of acivicin was superimposed on the same atoms of the trapped intermediate in CPS. Once again, the potential for charge stabilization by the oxyanion hole of the backbone NH for Leu 270 and Gly 241 was evident. This feature was also observed in models of acivicin in the glutaminase domain of AS (not shown). In every model, the (α*S*,5*R*) diastereomer docked with the dihydroisoxazole ring "flipped" in an orientation that projects the N−O bond away from the oxyanion hole while keeping the C3 imino carbon within bonding distance of the cysteine sulfur. This lack of potential charge stabilization leads to the low binding affinity exhibited by the (α*S*,5*R*) diastereomer.

Electrostatic potential maps of the acivicin models in the glutaminase active sites illustrate the complimentary features of the ligand and protein. As expected, models of acivicin using the AMBER force field indicate the N−O bond is a highly electronegative region that contributes to the polarization of the C3−C4 bond. In the GMPS glutaminase active site (Figure 8), the hydrophobic residues (Gly 59, Phe 83, Gly 84, Val 85, Tyr 87, and Gly 88) surrounding the N and O of the dihydroisoxazole ring provide an electropositive surface (red in color). This surface is complemented by the electronegative potential of the dihydroisoxazole ring (shown in purple). Upon cysteine attack of acivicin (or glutamine) to form the tetrahedral intermediate, charge stabilization would be enhanced by the electropositive and hydrogen bonding features of this active site. The electronegative character of the N−O bonding system in acivicin appears to be a mechanistic basis for the specificity of this compound for the glutaminase active sites. The relationship was also observed in the models of acivicin in CPS and AS. In this way, the electronics of the dihydroisoxazole ring presents a unique template for enzyme inhibitor design in related cysteine proteases.

In summary, many features of the acivicin inactivation of IGPS from *E. coli* and *S. cerevisiae* and GMPS are consistent with the current knowledge about the coordinate activity of the glutaminase and acceptor sites in these enzymes (*20*, *25*). Both of these enzyme systems have exhibited nucleotide substrate dependence on the rate of turnover for the glutaminase activity and these properties have been noted in the other triad GATs (*19*). Nucleotide substrates in the acceptor domains for either IGPS or GMPS result in increased specificity for acivicin as reflected in the comparisons of k_{inact}/K_i^{app} data. These increases in specificity reflect a shift to the inactivated enzyme complex in much the same way that glutamine would toward ammonia and glutamate. When considering the intracellular specificity of acivicin, these features are critical since both substrates are present. A structural basis to relate the oxyanion hole and catalytic triads in the glutamine binding sites with the critical dynamic features of the triad GATs is important for understanding the function of these enzymes as well as the design of any future glutamine antagonists. These efforts will depend on

further studies of the individual enzymes structures with bound ligands as they relate to the specific conformational states.

ACKNOWLEDGMENT

We thank Dr. Janet Smith and Dr. John Burgner for helpful discussions and suggestions.

REFERENCES

1. Colquhoun, A., and Newsholme, E. A. (1997) *Biochem. Mol. Biol. Intl. 41*, 583−596.
2. Medina, M. A., Quesada, A. R., and Nunez de Castro, I. (1991) *J. Bioenerg. Biomembr. 23*, 689−697.
3. Souba, W. W. (1993) *Ann. Surg. 218*, 715−728.
4. Prajda, N. (1985) *Adv. Enzyme Regul. 24*, 207−223.
5. Ahluwalia, G. S., Grem, J. L., Hao, Z., and Cooney, D. A. (1990) *Pharmacol. Ther. 46*, 243−271.
6. Huber, K. R., Rosenfeld, H., and Roberts, J. (1988) *Int. J. Cancer 41*, 752−755.
7. Lyons, S. D., Sant, M. E., and Christopherson, R. I. (1990) *J. Biol. Chem. 265*, 11377−11381.
8. Weber, G., and Prajda, N. (1994) *Adv. Enz. Regul. 34*, 71−89.
9. Hanka, L. J., and Dietz, A. (1973) *Antimicrob. Agents Chemother. 3*, 425−431.
10. Tso, J. Y., Bower, S. G., and Zalkin, H. (1980) *J. Biol. Chem. 255*, 6734−6738.
11. Krahn, J. M., Kim, J. H., Burns, M. R., Parry, R. J., Zalkin, H., and Smith, J. L. (1997) *Biochemistry 36*, 11061−11068.
12. Nakamura, J., Straub, K., Wu, J., and Lou, L. (1995) *J. Biol. Chem. 270*, 23450−23455.
13. Olver, I. N., Green, M., Millward, M. J., and Bishop, J. F. (1998) *J. Clin. Neurosci. 5*, 46−48.
14. Lui, M. S., Kizaki, H., and Weber, G. (1982) *Biochem. Pharmacol. 31*, 3469−3473.
15. Agarwal, R. P. (1994) *Biochem. Biophys. Res. Commun. 202*, 1524−1529.
16. Eisenhauer, E. A., Maroun, J. A., Fields, A. L., and Walde, P. L. (1987) *Invest. New Drugs 5*, 375−378.
17. Maroun, J. A., Stewart, D. J., Verma, S., Evans, W. K., and Eisenhauer, E. (1990) *Am. J. Clin. Oncol. 13*, 401−404.
18. Poster, D. S., Bruno, S., Penta, J., Neil, G. L., and McGovren, J. P. (1981) *Cancer Clin. Trials 4*, 327−330.
19. Zalkin, H., and Smith, J. (1998) *Adv. Enzymol. Related Areas Mol. Biol. 72*, 87−144.
20. Chittur, S. V., Chen, Y., and Davisson, V. J. (2000) *Prot. Express. Purif. 18*, 366−377.
21. Tesmer, J. J. G., Klem, T. J., Deras, M. L., Davisson, V. J., and Smith, J. L. (1996) *Nat. Struct. Biol. 3*, 74−86.
22. Knochel, T., Ivens, A., Hester, G., Gonzalez, A., Bauerle, R., Wilmanns, M., Kirschner, K., and Jansonius, J. N. (1999) *Proc. Natl. Acad. Sci. U.S.A. 96*, 9479−9484.
23. Thoden, J. B., Miran, S. G., Phillips, J. C., Howard, A. J., Raushel, F. M., and Holden, H. M. (1998) *Biochemistry 37*, 8825−8831.
24. Thoden, J. B., Holden, H. M., Wesenberg, G., Raushel, F. M., and Rayment, I. (1997) *Biochemistry 36*, 6305−6316.
25. Klem, T. J., and Davisson, V. J. (1993) *Biochemistry 32*, 5177−5186.
26. Halling, K., Thomsen, I., and Torssell, K. B. G. (1989) *Liebigs Ann. Chem.*, 985−990.
27. Mzengeza, S., and Whitney, R. A. (1988) *J. Org. Chem. 53*, 4074−4081.
28. Silverman, R. B., and Holladay, M. W. (1981) *J. Am. Chem. Soc. 103*, 7357−7358.
29. Press, W. H., Flannery, B. P., Teukolsky, S. A., and Vetterling, W. T. (1993) *Numerical Recipes in C: The Art of Scientific Computing*, 2nd ed., Cambridge University Press, Cambridge.
30. Kitz, R., and Wilson, I. B. (1962) *J. Biol. Chem. 237*, 3265−3269.
31. Gray, P. J., and Duggleby, R. G. (1989) *Biochem. J. 257*, 419−424.
32. Cleland, W. W. (1967) *Adv. Enzymol. Related Areas Mol. Biol. 29*, 1−32.
33. Andrews, P. C., and Dixon, J. E. (1987) *Anal. Biochem. 161*, 524−528.
34. Elliott, W. L., and Weber, G. (1985) *Biochem. Pharmacol. 34*, 243−248.
35. Zalkin, H., and Truitt, C. (1977) *J. Biol. Chem. 252*, 5431−5436.
36. Deras, M. L., Chittur, S. V., and Davisson, V. J. (1999) *Biochemistry 38*, 303−310.

BI0014047